Trans. JWRI, Vol. 24 (1995), No. 2

Establishment of Computational Welding Mechanics†

Yukio UEDA*, Hidekazu MURAKAWA**, Keiji NAKACHO*** and Ning Xu MA***

Abstract

The authors have been engaged in the development of numerical methods for the analysis of mechanical processes in welding for the last three decades. Due to the great advances in numerical methods such as the FEM and the computer technologies , numerical methods in this field have reached the stage to establish computational welding mechanics. In this paper, the history of computational welding mechanics is reviewed. Also, the current research activities by the authors are summarized. Analyses of residual stresses and distortions in welding and cutting, measurement of three dimensional distribution of residual stresses and computation of weldability lobes for spot welding are presented as examples.

KEY WORDS: (Computation) (Numerical Method) (Finite Element Method) (Welding) (Residual Stress) (Distortion)

1. Introduction

The authors are establishing a new Welding Mechanics as a Computational Science by developing new methods for the evaluation of welding stress and strain in two and three dimensions with the aid of FEM. In this paper, the authors will describe their essential approaches for theoretical analysis, prediction and measurement of welding residual stresses and distortions. The three approaches are;

(1) method of thermal elasto-plastic analysis with the effect of creep
(2) prediction of welding residual stress using inherent strain (the source of residual stress) through elastic analysis
(3) measuring method using inherent strain as a parameter.

Method (1) using FEM[1] was proposed in 1971. The proposed method can take into account various influencing factors, such as temperature dependent material properties and geometrical nonlinearity. Method (2) consists of inverse calculation of inherent strain from numerical and experimental residual stresses and prediction of welding residual stress by elastic analysis[2]. Thus, it becomes possible to predict the residual stress in large structures by simple elastic computation. Method (3) enables us to measure three dimensional residual stress without any approximation[3].

Various examples of these approaches will be demonstrated, which clarify the mechanism of the production of welding residual stresses, the relation between the restraint intensity and residual stress/strain, mechanical criteria of weld cracking, etc.

2. Histories of Computational Welding Mechanics

Important concepts in welding mechanics were established quite early based on analytical investigations. In Japan, Profs. T. Naka, T. Okumura[4], M. Otani[5] ,M. Watanabe and K. Satoh[6] were the pioneers in this field. The invention of digital computers and the development of numerical methods such as the Finite Element Methods during the 1970's made it possible to begin a new phase of welding mechanics. That is the computational welding mechanics. Active researches were carried out by two or three research groups in Japan including the authors'.

† Received on Nobember 24, 1995
* Professor
** Associate Professor
*** Assistant Professor
**** Research Associate
Transactions of JWRI is published by Welding Research Institute of Osaka University, Ibaraki, Osaka 567, Japan.

The authors' first work on the computational welding mechanics was presented as an IIW Document[1] in 1971. The proposed model was a Thermal-Elastic-Plastic one. One of the most important assumptions was that : the total strain increment can be separated into the sum of the elastic, the plastic and the thermal strain increments. Also, plastic flow theory was assumed to be applicable to the plastic deformation, i.e.,

$$\Delta\varepsilon_{ij} = \Delta\varepsilon^{e}_{ij} + \Delta\varepsilon^{p}_{ij} + \Delta\varepsilon^{T}_{ij} \quad (1)$$

$$\Delta\varepsilon^{p}_{ij} = \lambda(\partial f/\partial\sigma_{ij}) \quad (2)$$

where, $\Delta\varepsilon_{ij}$, $\Delta\varepsilon^{e}_{ij}$, $\Delta\varepsilon^{p}_{ij}$ and $\Delta\varepsilon^{T}_{ij}$ are the total, the elastic, the plastic and the thermal strain increments, respectively, and f is the plastic potential. The theory was implemented as the Finite Element Method.

The problems solved at that time were rather simple. But, two dimensional problems under moving heat sources were already studied. **Figure 1** shows the Finite Element mesh division used for the computation and the computed transient thermal stress under a moving heat source is shown by **Fig.2**. Another problem studied was the mechanical behavior of rigidly restrained weld cracking test specimen as shown by **Figs.3** and **4**.

The FEM was soon applied to multi-pass welding problems. **Figure 5** shows a multi-pass welding problem in a pressure vessel[7]. This problem was idealized as a two dimensional model as illustrated in **Fig.6**. The computed through thickness distributions of

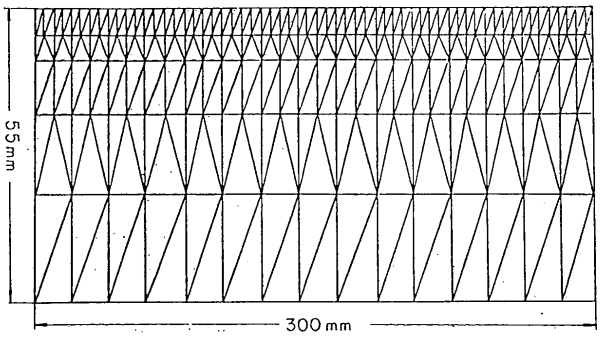

Fig.1 Idealization of half of plate subjected to a moving heat source.

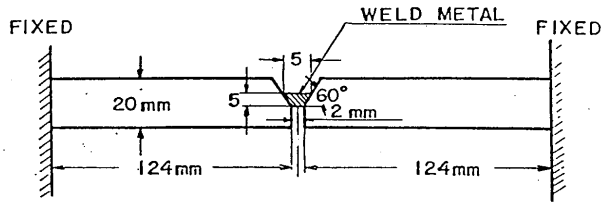

Fig.3 Rigidly restrained weld cracking test specimen.

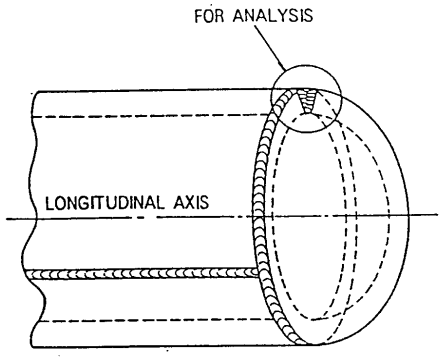

Fig.5 Welded cylinder-head connection of a pressure vessel.

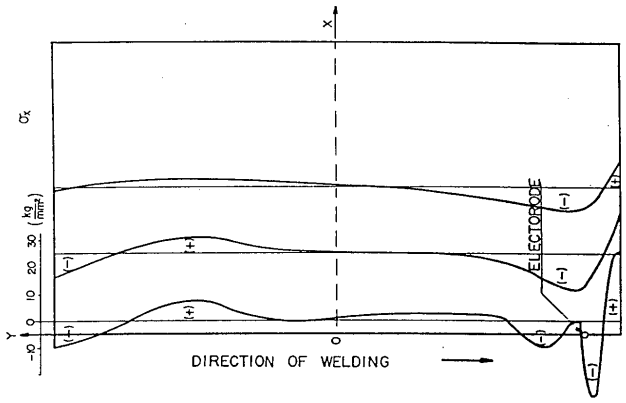

Fig.2 Transient thermal stress σ_X under a moving heat source.

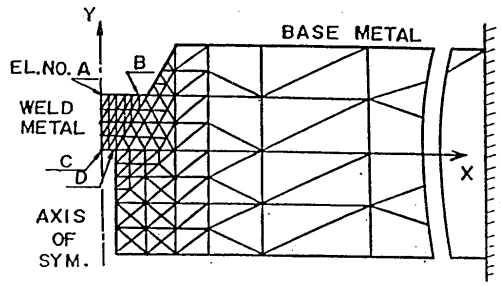

Fig.4 Finite Element mesh division of specimen.

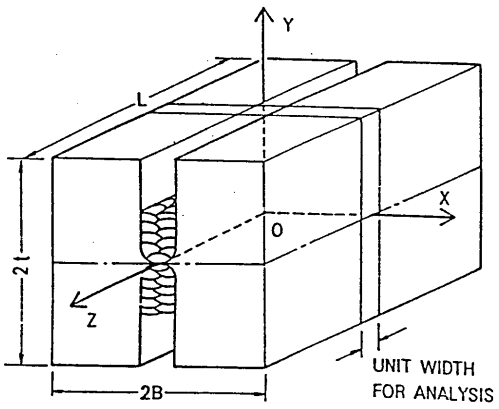

Fig.6 Idealized computational model.

the residual stress after the welding of each layer are presented in **Fig.7**. It is seen that the maximum residual stress appears just below the surface of the final layer.

The FEM was also applied to investigate the effectiveness of the heat-sink method[8] to reduce the residual stress on the inner surface of a pipe. The heat-sink method involves welding with the inner pipe surface cooled by a water flow as shown by **Fig.8**. As the computed results in **Figs.9** and **10** show, the residual stress with conventional welding is tensile at the welded part. It becomes compressive, when the heat-sink method is used.

Cracking problems are very important in welding mechanics. The mechanical behavior of the slit weld specimen, which is shown in **Fig.11**, was analyzed using the FEM[9]. The relationship between the characteristics of the stresses and strains in the slit

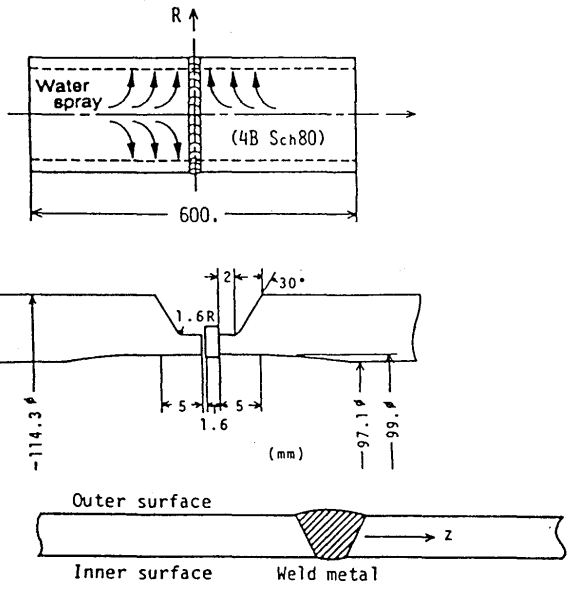

Fig.8 Heat-sink method.

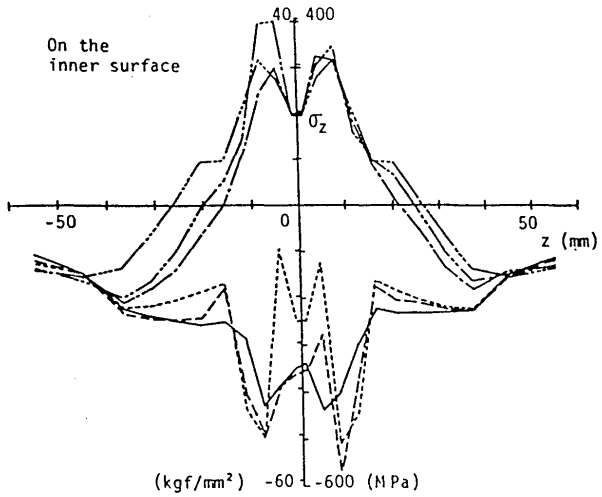

Fig.10 Distribution of residual stress in transverse direction.

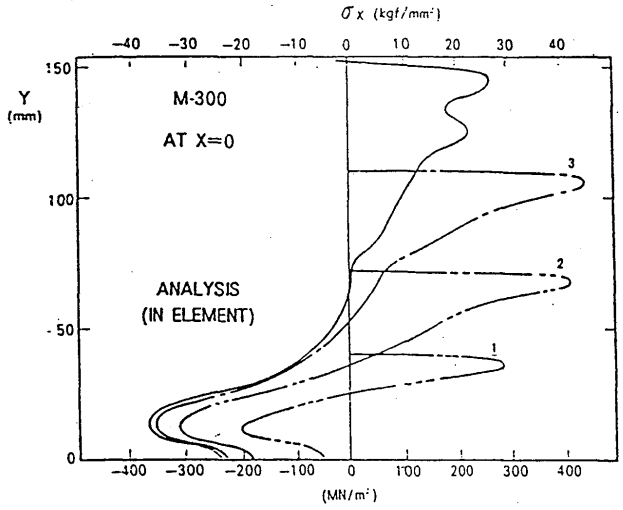

Fig.7 Transient transverse welding stress σ_x at the cross-section (x=0).

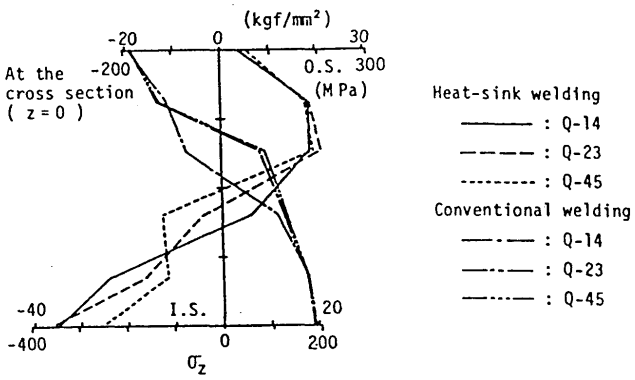

Fig.9 Through thickness distribution of residual stress.

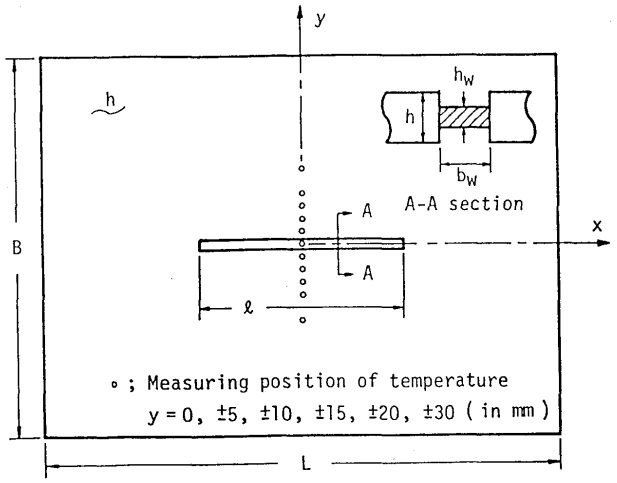

Fig.11 Slit weld specimen.

specimen and the magnitude of heat input are summarized in **Fig.12.**

3. Inherent Strain in Computational Mechanics

The Finite Element Method alone is just a numerical method. It is also necessary to have a conceptual backbone for the consistent understanding of the phenomena and the better usage of the computational method. This is provided by the concept of inherent strain. When it is combined with the FEM, computational welding mechanics becomes truly attractive and useful.

Inherent strain is the strain which produces both welding residual stress and welding distortion. The concept of inherent strain is very useful for the following reasons;

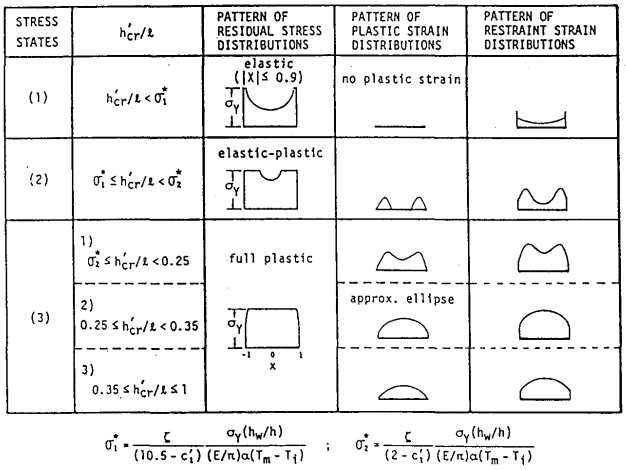

Fig.12 Restraint intensity and restraint stress-strain in slit weld.

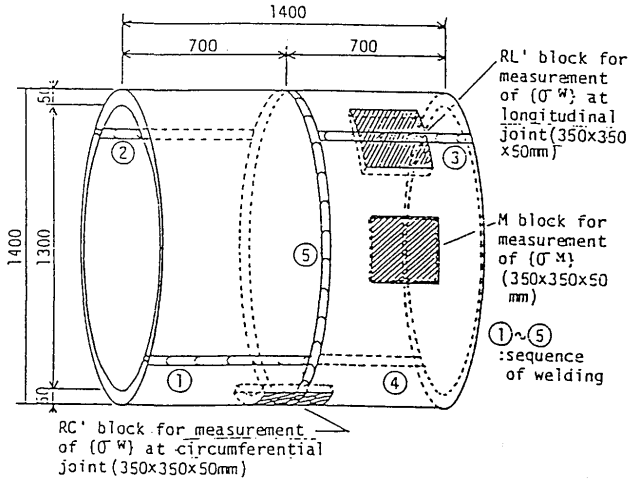

Fig.13 Model of pen-stock.

(1) It helps the understanding of the mechanism which produces the welding residual stress and distortion.
(2) It can be used for the measurement of the three dimensional residual stress.
(3) Once the inherent strain is known, the residual stress and the distortion can be computed by elastic analysis.
(4) In the assessment of the effect of the welding residual stress and the distortion on the strength and the reliability of structures, inherent strain is the ideal physical value to describe the problem.

When the distribution of inherent strain is described by a finite number of parameters $\varepsilon^*_1, \varepsilon^*_2, \varepsilon^*_3, \cdots\cdots$, the residual stresses $\{\sigma_i\}$ and the elastic strains $\{\varepsilon^e_i\}$ at arbitrary points in a welded joint or a structure can be considered as function of these parameters, i.e.,

$$\varepsilon^e_i = \varepsilon^e_i(\varepsilon^*_1, \varepsilon^*_2, \varepsilon^*_3, \cdots\cdots) \quad (3)$$

$$\sigma_i = \sigma_i(\varepsilon^*_1, \varepsilon^*_2, \varepsilon^*_3, \cdots\cdots) \quad (4)$$

If the deformation caused by the inherent strain is small, the elastic strains $\{\varepsilon^e_i\}$ and the residual stresses $\{\sigma_i\}$ are linear functions of the inherent strains, i.e.,

$$\{\varepsilon^e_i\} = [H_{ij}]\{\varepsilon^*_j\} \quad (5)$$

$$\{\sigma_i\} = [D][H_{ij}]\{\varepsilon^*_j\} \quad (6)$$

If these elastic strains are measured through experiments, the inherent strain can be determined as an inverse problem using Eq.(5). The matrix $[H_{ij}]$ in Eq.(5) relating the measured strain and the inherent strains can be obtained using FEM. It is important to emphasize that the inherent strain does not change or disappear by cutting and this is the reason why it can be used in the measurement of three dimensional residual stress. In case of elastic strain or stress, these change with cutting.

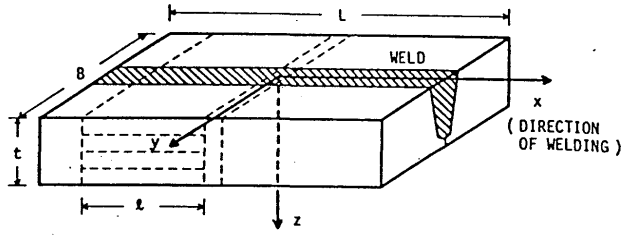

(a) Experimental model of multi-pass welded joint (R-specimen)

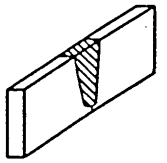

(b) Sliced cross section in the weld line (T-specimen)

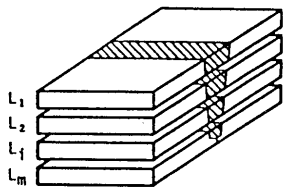

(c) Sliced plates, parallel to xy-plane (Li-specimen)

Fig.14 Procedure of residual stress measurement using T and L_i sliced specimens.

4. Examples of Researches Using FEM and Inherent Strain

The first example is the residual stress measurement in a thick welded cylinder[10] which is shown in **Fig.13**. Since the inherent strain does not change by cutting, the specimen can be cut into thin sliced specimen to measure three-dimensional residual stress using strain gages. Thin specimens, such as the T-specimen and Li-specimens shown in **Fig.14**, are cut out to measure the elastic strain. From the measured elastic strain, the inherent strains are determined. The residual stress in the original three-dimensional structure can be reconstructed using FEM and the inherent strain. **Figures 15** and **16** show the through thickness distributions of the residual stress at the longitudinal and the circumferential joints. The macro-photographs of these joints are shown in **Fig.17**.

The second example is the prediction of the residual stress in built-up T and I-sections[11] shown in **Fig.18**.

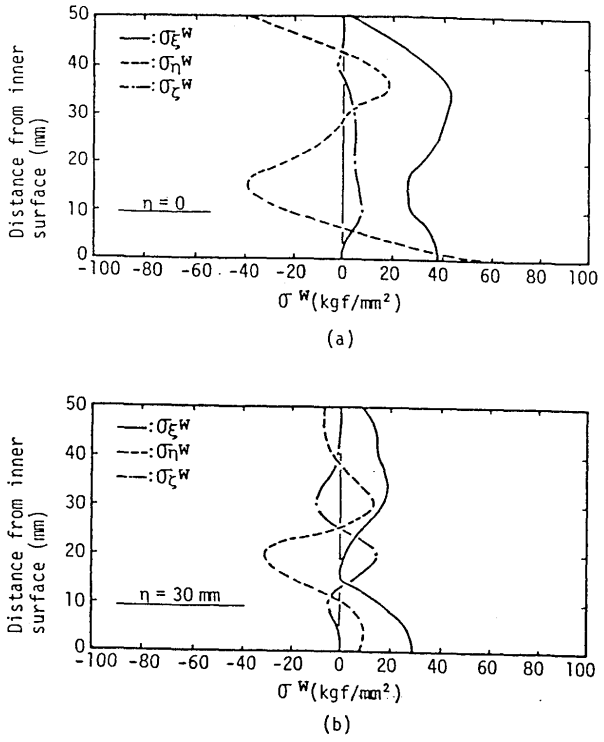

Fig.15 Welding residual stresses at the longitudinal joint.

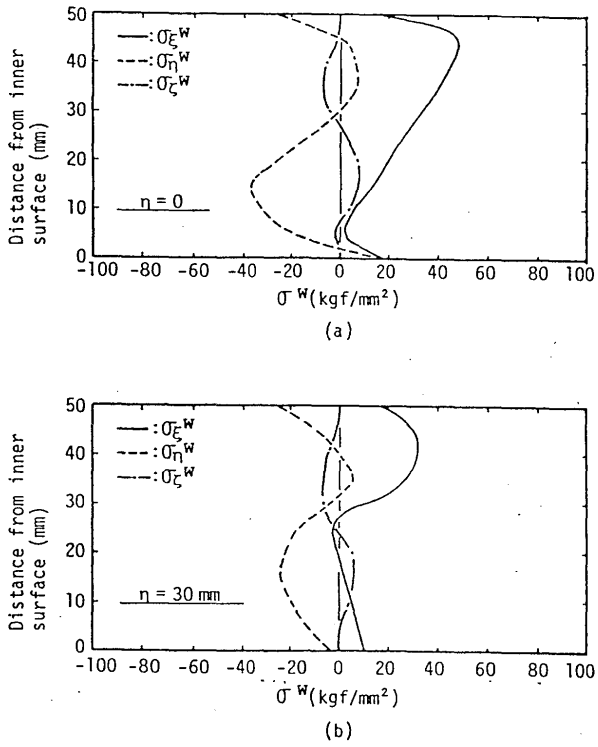

Fig.16 Welding residual stresses at the circumferential joint.

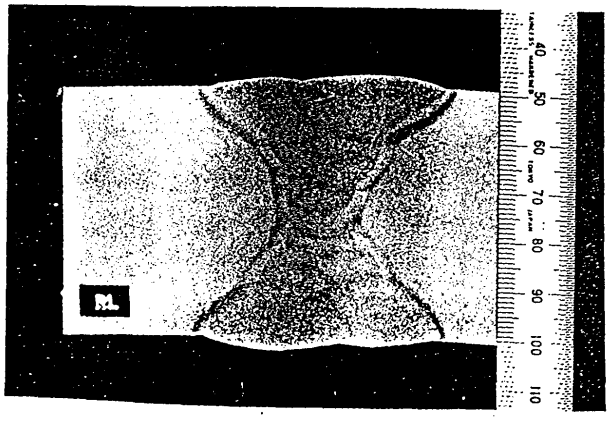

(a) Longitudinal joint

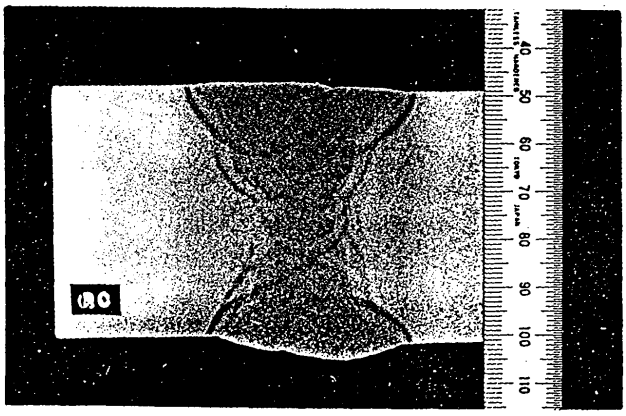

(b) Circumferential joint

Fig.17 Macro-photographs of weldments.

If the inherent strain for each welding line is known, the residual stress distribution in the built up section can be computed by elastic FEM. In this prediction, the effect of the welding sequence can be considered as illustrated in Fig.19. Thus, differences in the residual stresses at the top and the bottom flanges of the I-section are correctly reproduced as seen in Fig.20, which shows the comparison between the residual stresses computed by the thermal-elastic-plastic FEM and those predicted using the inherent strain.

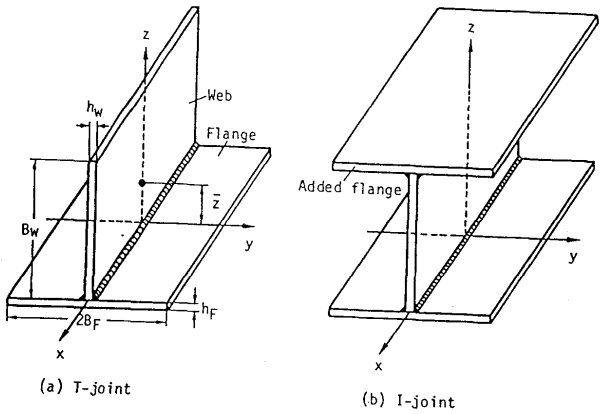

Fig.18 Fillet welded joints.

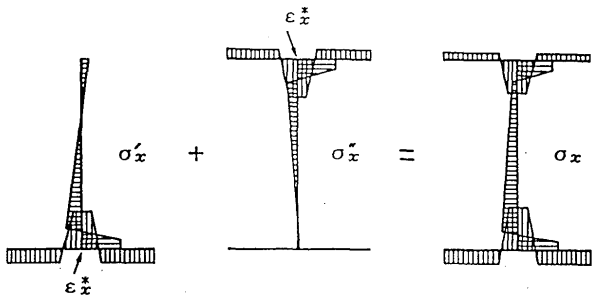

Fig.19 Process of predicting residual stress in I-joint using inherent strain.

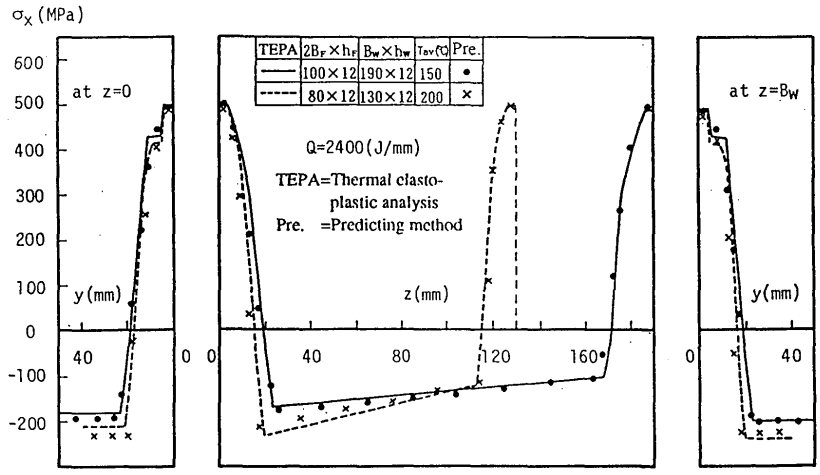

Fig.20 Comparison of residual stresses in I-joints obtained by proposed method and by thermal-elastic-plastic analysis.

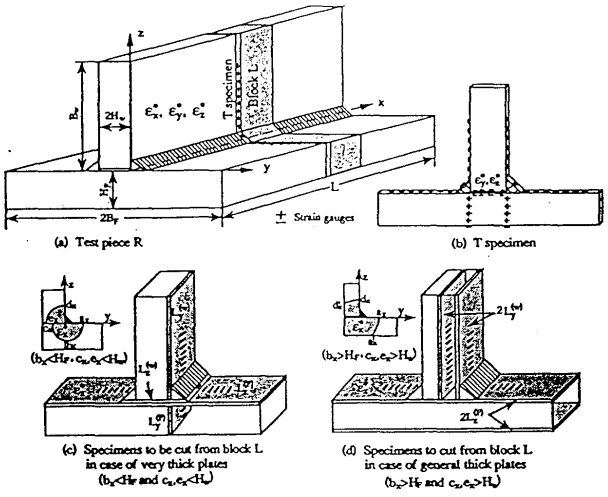

Fig.21 Fillet weld and sliced specimens used in the measurement of residual stresses.

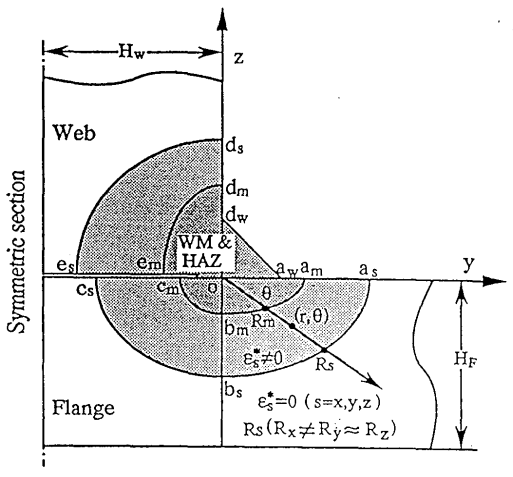

Fig.22 Elliptical distribution zone of inherent strain in a fillet weld.

The inherent strain can be also applied to the measurement of residual stress in fillet welds[12]. The procedure of measurement is shown in **Fig.21**. The regions where the inherent strain exists can be separated into two elliptical regions as shown in **Fig.22**. The assumed distributions of the inherent strains in the radial and the circumferential directions are shown in **Fig.23**. The radii of the ellipses R_m and R_s, and the magnitudes of inherent strain ε^*_{s0}, ε^*_{sRm}, ····· are the parameters defining the inherent strain distribution. These parameters are determined through the inverse problem using the small number of measured elastic strains as input data. The residual stress reproduced by the inherent strain and directly measured stresses on the surface are shown in **Fig.24**. The maximum transverse stress σ_y is observed near the toe of the welding.

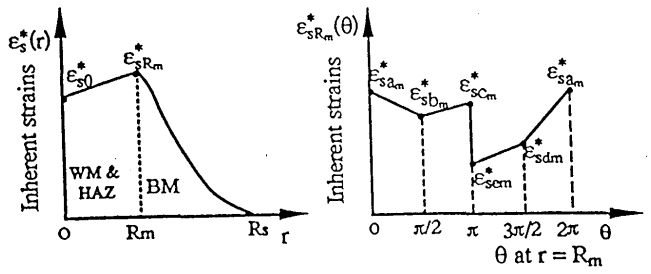

Fig.23 Distribution pattern of inherent strains.

The residual stresses in explosively clad steel plates are measured using the FEM and inherent strain[13]. The clad plate consists of four layers as shown in **Fig.25**.

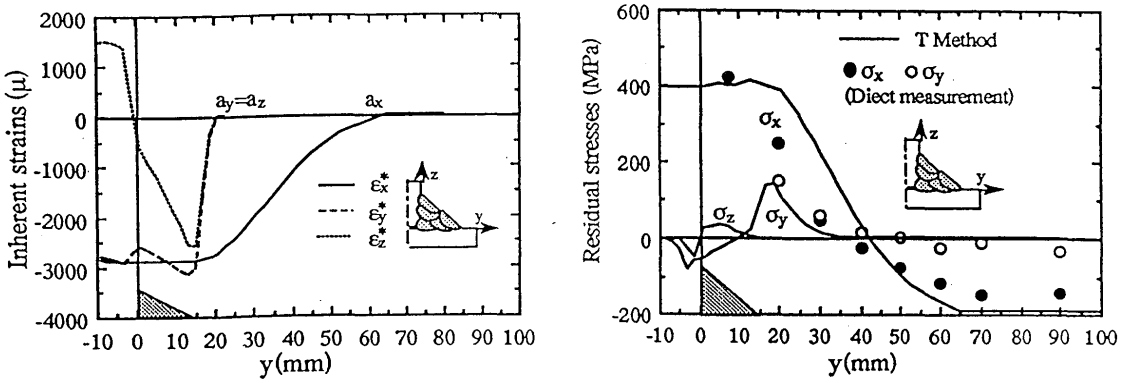

Fig.24 Estimated inherent strain and residual stress distributions in T-type fillet weld.

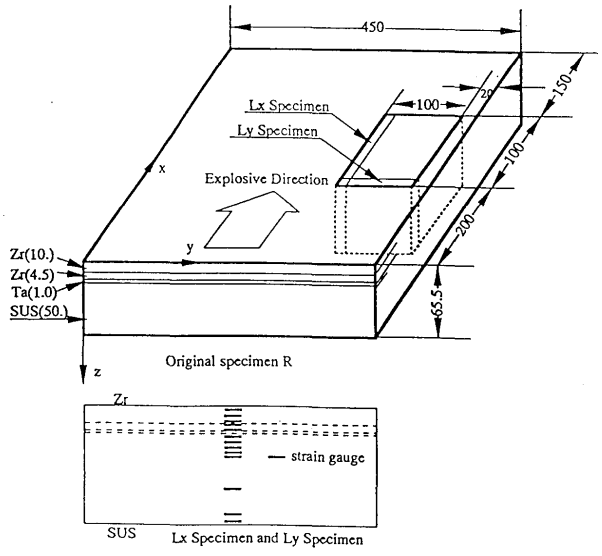

Fig.25 Zr/Zr/Ta/SUS304 clad plate and specimens used in the measurement of residual stress.

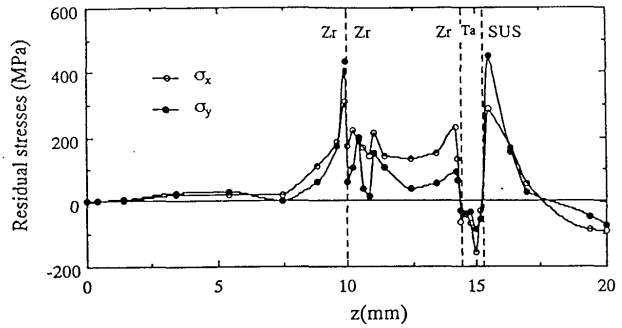

Fig.26 Through thickness distributions of residual stresses.

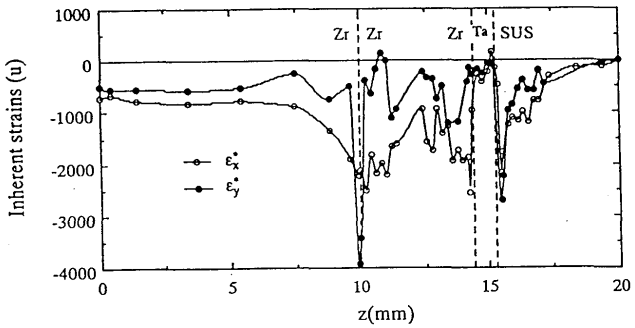

Fig.27 Through thickness distributions of inherent strains.

The measured residual stresses are shown in **Fig.26**. The distributions of the corresponding inherent strains are shown in **Fig.27**. Once the inherent strain is known, the residual stress, when a cylindrical part is cut out from the clad plate, can be computed using the inherent strain as shown in **Figs.28** and **29**.

To study the effect of welding residual stress and distortion on the performance of welded structures, the concept of inherent strain is very useful. **Figure 30** shows a typical example of stiffened plates commonly found in steel structures. The residual stress due to welding can be estimated using the inherent strain according to the size of the plate[11]. The effect of the welding deformation which involves various mode shapes can be taken into account through an equivalent uni-modal initial deformation[14]. **Figure 31** shows the effect of the residual stress and the initial deflection on the compressive ultimate strength of rectangular plates. Similarly, their influence on the strength of the stiffened plates[15] are summarized in **Figs.32** and **33**.

5. Current Research Topics in Computational Welding Mechanics

One of the significant differences between the researches in the 1970-80's and those in the 90's is the scale and the precision of the models. Due to the great advances in computer technology, large scale nonlinear transient problems can be solved on work stations. This makes it possible to analyze the real model rather than the scaled or simplified experimental model and gives special advantages to computational mechanics compared with physical experiments. The advantages of computational welding mechanics over the experiments are,

(1) The size of the model and the welding conditions are not subjected to physical limitations of apparatus.
(2) Cost may be less than experiments.

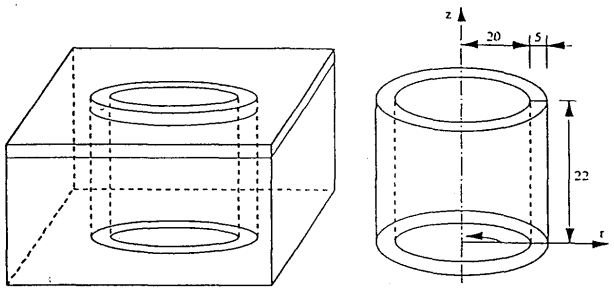

Fig.28 Pipe joint piece cut from Ni/SUS clad plate.

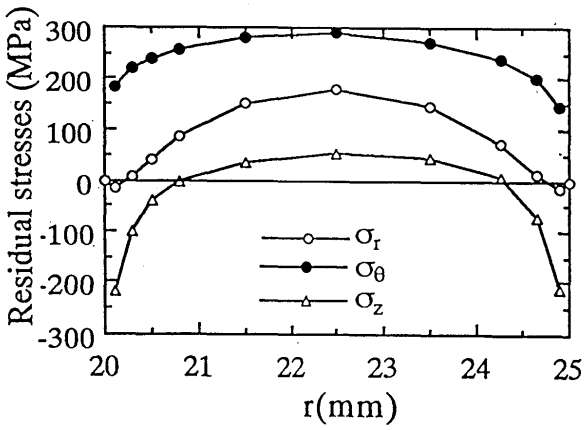

Fig.29 Residual stress in pipe joint piece cut from Ni/SUS clad plate.

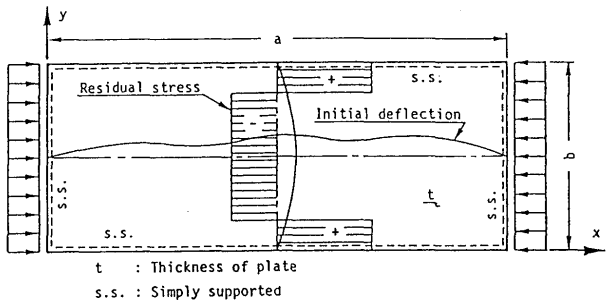

(a) Long rectangular plate with welding residual stresses and initial deflection

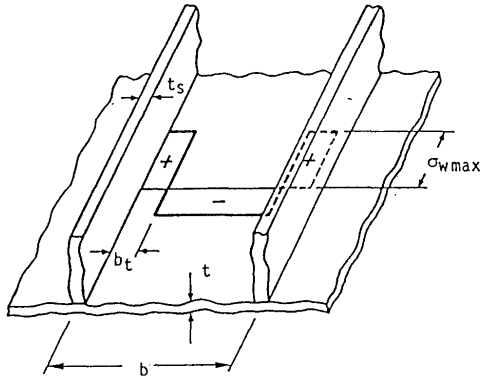

(b) Distribution of residual stresses due to welding of longitudinal stiffeners

Fig.30 Typical model of a welded stiffened panel under compression.

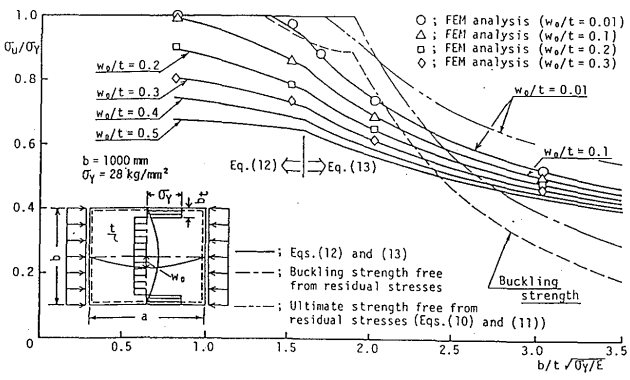

Fig.31 Compressive ultimate strengths of rectangular plates with uni-modal imperfections.

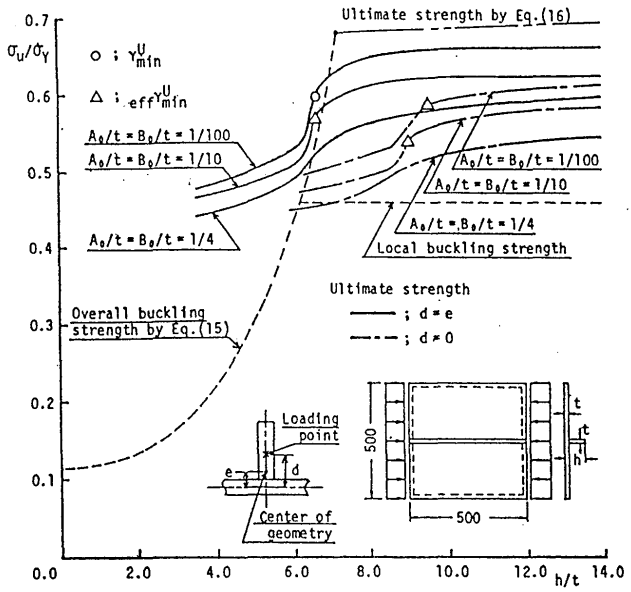

Fig.32 Influence of initial deflection on compressive ultimate strength of one-sided stiffened plates.

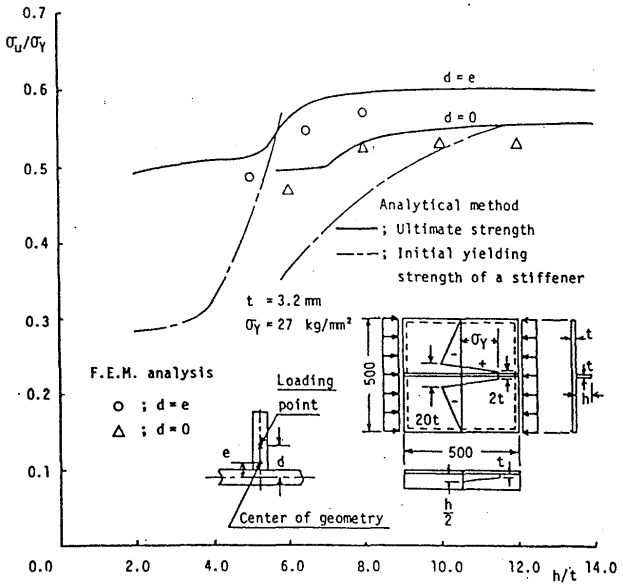

Fig.33 Influence of welding residual stress on compressive ultimate strength of one-sided stiffened plates.

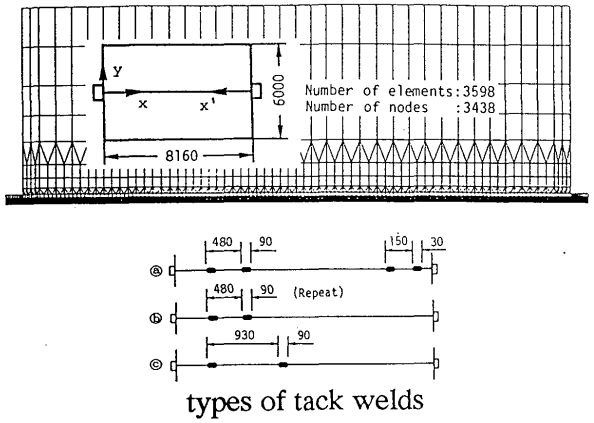

Fig.34 FEM model of butt welding of ship plates.

Table 1 Type of root gaps and methods to correct them.

Type	Before tack welding	Size of gap	Procedure of correction
Middle-gap		About 5 mm	Heat shaded areas. Weld tacks right after gas heating. Close the gap up to about 2-3 mm.
		2-3 mm	Weld tacks from the ends to the middle of the gap. Close the gap up to 1-2mm.
End-gap		About 5 mm	Heat shaded areas. Weld tacks after the plate is cooled down. Close the gap up to about 2-3 mm.
		2-3 mm	Weld tacks from the middle to the ends of the gap. Close the gap up to 1-2mm.
Double-gap			Weld tacks from the place in contact to the middle of gap. Close the gap up to 2-3 mm.

(3) Information which is not physically measurable can be obtained.

(4) Ideal conditions can be easily simulated. Thus, computational welding mechanics is effective for identifying the influential factors.

For automation or when robots are introduced in welding, the precision of preceding welding must be maintained. The first example is the identification of the influential factors in transverse welding deformation in butt welding of ship plates[16]. The size of the plate is 8 m by 6 m as shown in **Fig.34**. The details, such as the tack weldings and the tab plates are considered. From the computations and assuming different intervals for tack welds and different types of tab plate, the effect of the differences in tack and tab plate are found to be very small. Another suspected factor is the geometrical error due to cutting. When a large root gap is found, it is closed before welding by proper methods such as the choice of tack weld sequence or thermal deformation by gas heating as shown in **Table 1**. The effect of the initial gap on welding deformation in the transverse direction is shown by **Fig.35**. The line with solid circles represents the case with initial gap and the simple solid line corresponds to that without the gap. It is seen that the effect of the initial gap is very large. This suggests that the accuracy of cutting must be maintained.

The out-of-plane deformation of the plate due to the butt welding is also analyzed by considering the contact between the plate and the working table under gravitational force[17]. In this study the effectiveness of

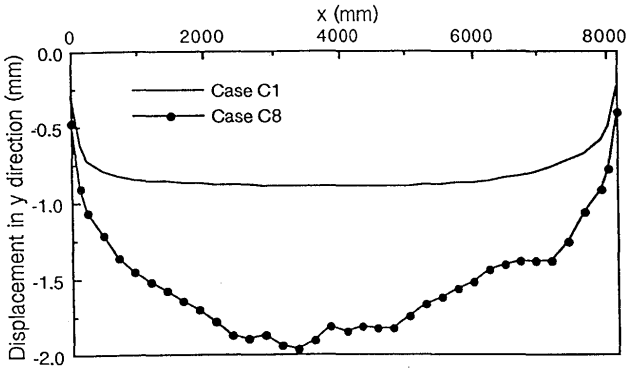

Fig.35 Welding deformation considering the residual stress and deformation due to correcting a gap by gas heating.

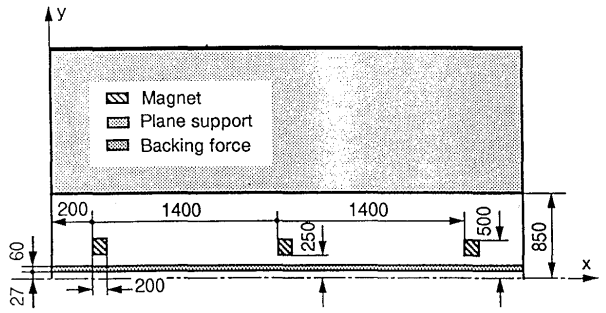

Fig.36 Magnetic constraint on plates used in shipyards.

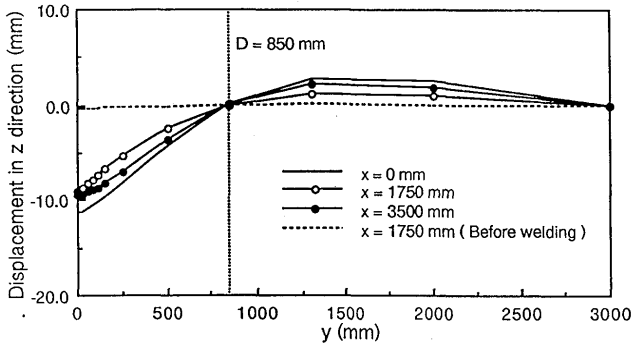

Fig.37 Out of plane deformation of plate due to butt welding without constraint.

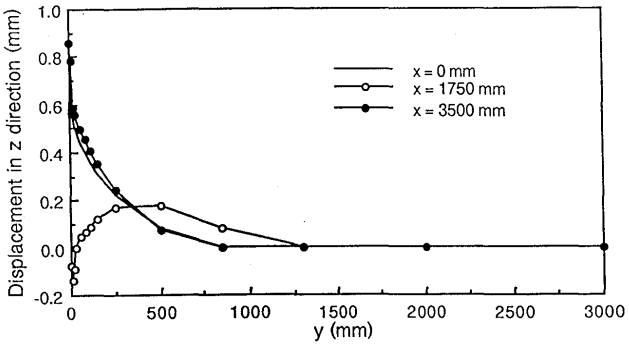

Fig.38 Out of plane deformation of plate due to butt welding with constraints by magnets.

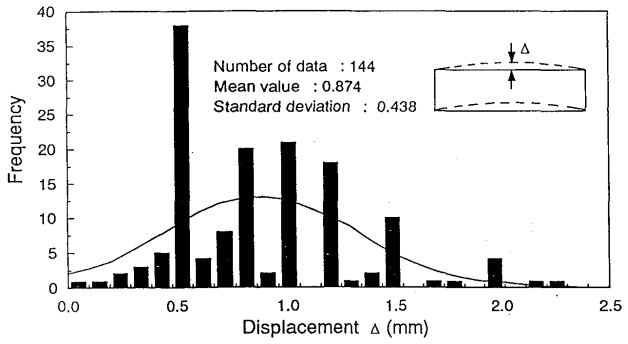

Fig.39 Statistical distribution of the measured maximum error along cut edges.

Table 2 Pattern of edge shape after gas cutting.

Type	Patterns of edge shape	Remark	Frequency
1		fan-shape	2 6
2		s-shape	1 5
3		partial s-shape	1 1
4		anti-barrel -shape	6
5		irregular local error (one side)	5
6		irregular local error (both sides)	9

the constraint by the magnets as shown in **Fig.36** is examined. The welding deformations with and without the constraint are compared in **Figs.37** and **38.**

The same thermal-elastic-plastic FEM which is used for welding problems can be applied to thermal cutting problems[18]. **Figure 39** and **Table 2** show the statistics of cutting errors observed in a ship yard. The error can be as much as 2 mm. To find out the influential factor in the cutting error, FEM is used as shown in **Fig.40**. To confirm the validity of the FEM, the deformation and the residual stress of a plate cut by air-plasma are computed and compared with the measured values in **Fig.41** and **Fig.42**. For both the deformation along the cutting line and the residual stress, the accuracy of FEM is satisfactory. The cutting error

can be separated into two parts. One is the deviation of the torch from the cutting line due to the transient thermal deformation, δ_{sy}. The other is the deformation caused by the residual plastic strain, δ_{dy}. **Figures 43** and **44** show the difference between two-sided simultaneous cutting and one-side cutting and the effect of supports on the cutting error.

Welding deformation is very critical for the mechanical parts of rotational machines in which high precision is required. The FEM can be applied to analyze the welding deformation of complex machine parts, such as the bearing of a compressor[19] shown in **Fig.45**. **Figure 46** shows the distribution of the welding residual stress. The three dimensional view of the computed welding deformation and the comparison with the measurement are presented in **Fig.47**. Through such computations, the factors influential in the welding deformation can be identified.

Resistance spot welding is slightly different from arc welding. However, it also can be analyzed by FEM[20] if the electric field, the thermal field and the displacement field are considered together with the change of contact state, as shown by the flowchart in **Fig.48**. As an example, dome-type and R-type electrodes which are shown in **Figs. 49** and **50** are considered. **Figures 51** and **52** show the time histories of the highest temperature at the nugget. From these computations, weldability lobes shown in **Figs. 53** and **54** can be drawn. Thus, the performance of the electrodes can be predicted without experiments.

The FEM and the concept of inherent strain can be also applied to plate bending by line heating. In ship yards in Japan, line-heating or flame bending is widely used to form curved plate. FEM can be used to predict the deformation caused by the line heating with given heating conditions. If it is used in the inverse manner, instructions on where and how to heat the plate to achieve the desired curved shape can be generated[21].

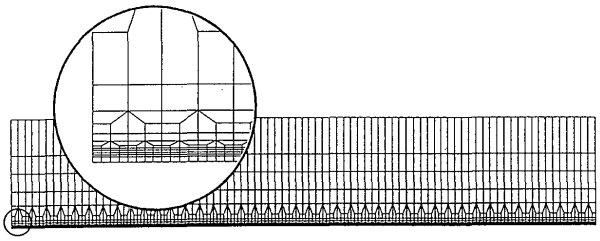

Fig.40 FEM model for plasma cutting.

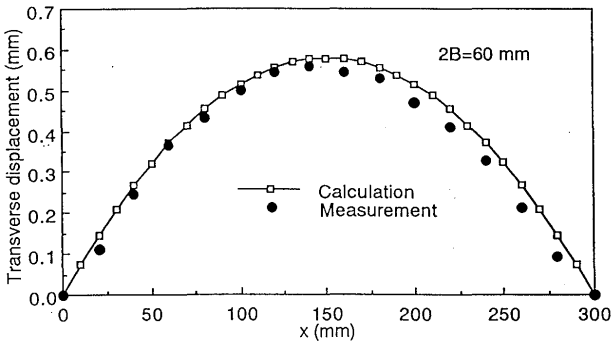

Fig.41 Measured and computed cutting deformations.

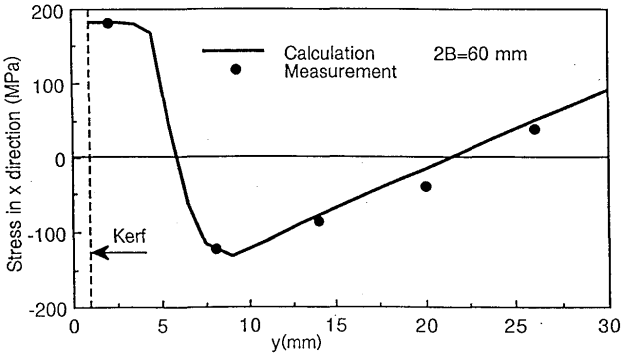

Fig.42 Distribution of residual stress in cutting direction.

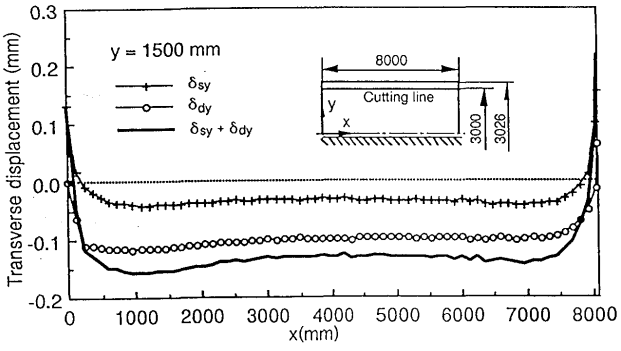

Fig.43 Distribution of cutting error (two-side simultaneous cutting).

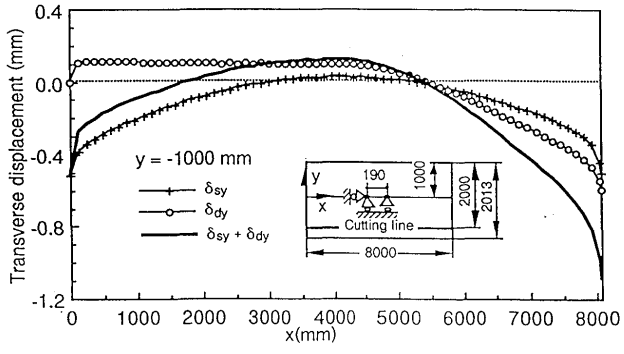

Fig.44 Distribution of cutting error (one-side cutting).

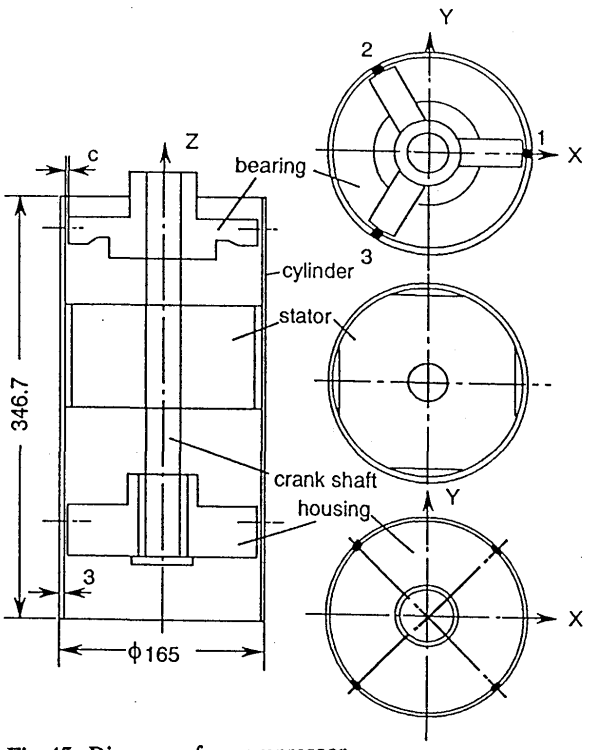

Fig.45 Diagram of a compressor.

6. Conclusions

As seen from various examples, there is no doubt about the importance and the usefulness of computational welding mechanics. To promote the techniques, development of advanced software packages and computers are very important, but they are not enough. It is also necessary to address the meaning of the computed results or their value in technological research. To extract the meaning or the value, the researchers or the engineers must have a genuine insight into the phenomena. Such insight can be acquired through the education based on the fundamental concepts established as classical welding mechanics.

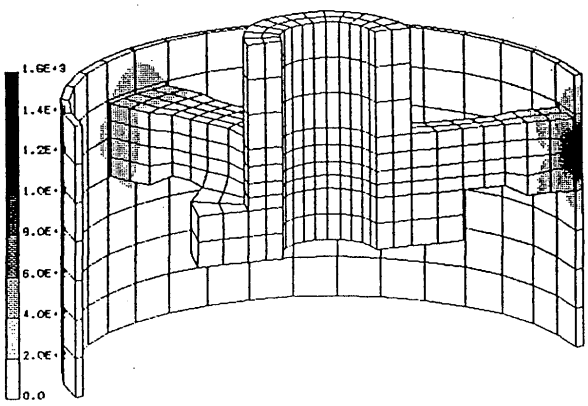

Fig.46 Distributions of residual stresses.

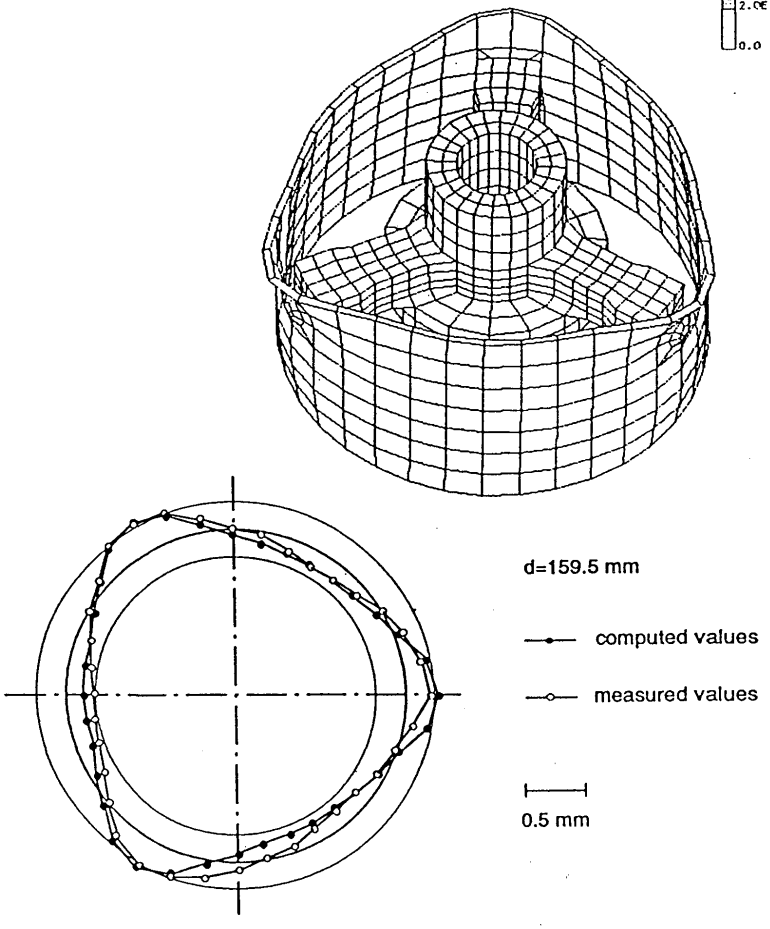

Fig.47 Computed and measured "flower pattern" deformations.

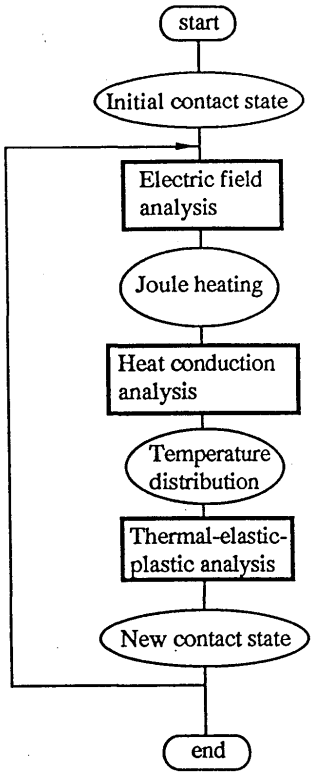

Fig.48 Flowchart of computation for spot welding.

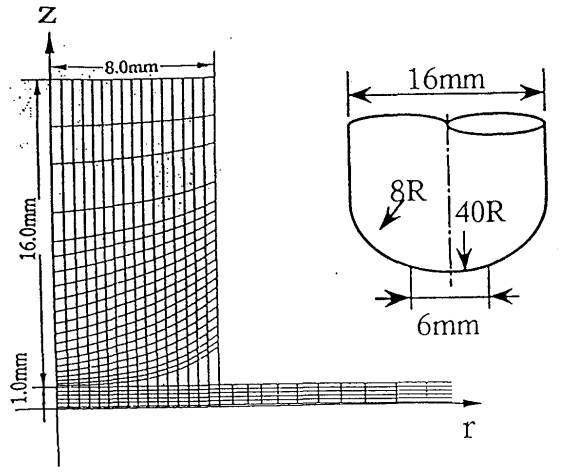

Fig.49 FEM mesh division for dome-type electrode.

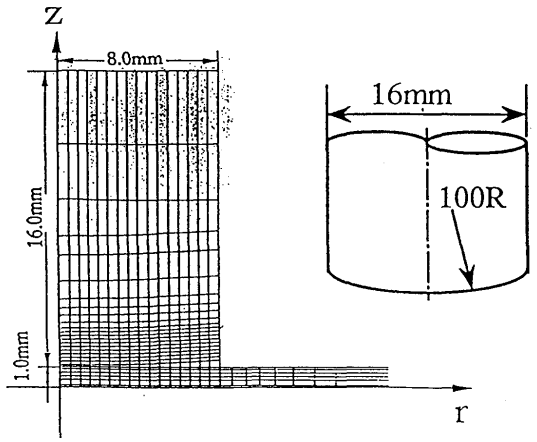

Fig.50 FEM mesh division for R-type electrode.

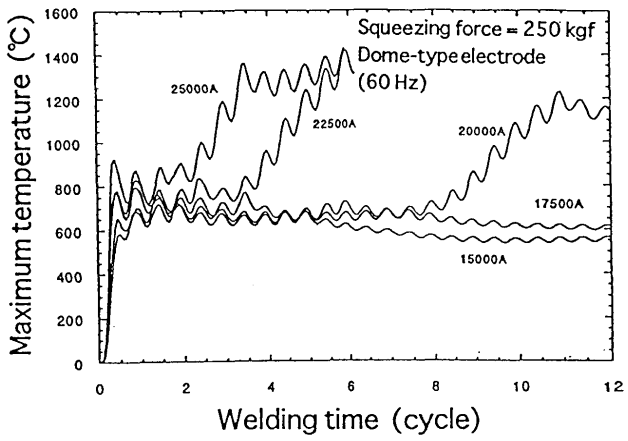

Fig.51 Time history of the highest temperature in welded zone (dome-type).

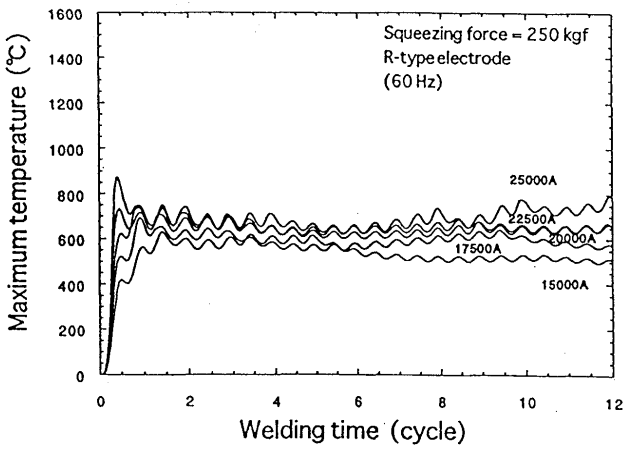

Fig.52 Time history of the highest temperature in welded zone (R-type).

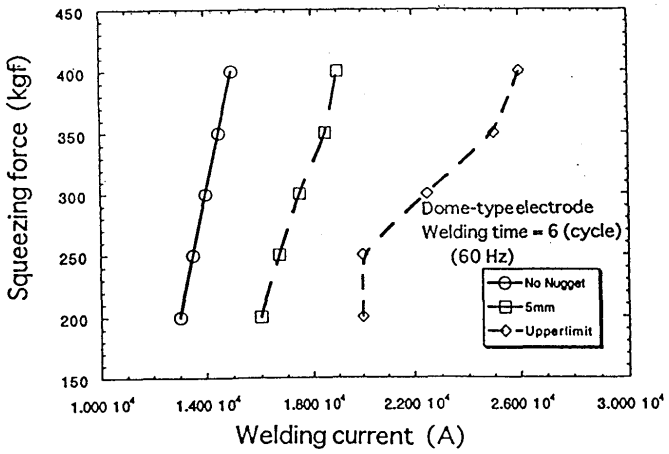

Fig.53 Computed weldability lobe for dome-type electrode.

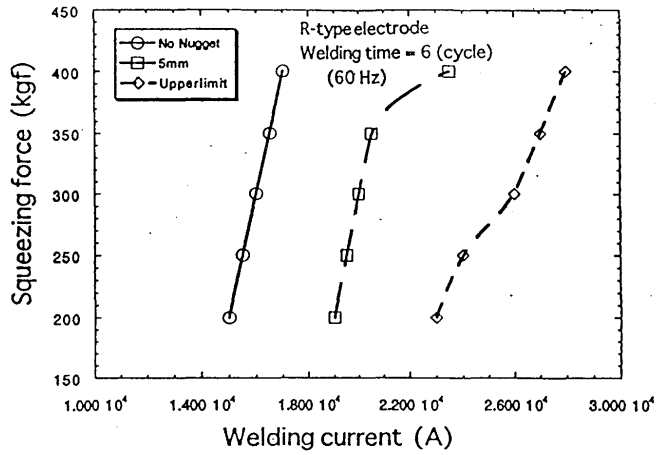

Fig.54 Computed weldability lobe for R-type electrode.

References

1) Y. Ueda and T. Yamakawa, "Analysis of Thermal Elastic-Plastic Stress and Strain during Welding", IIW Doc. X-616-71(1971), also Trans. Japan Welding Soc., Vol.2 (1971), No.2, 90-100.
2) Y. Ueda, K. Fukuda, K. Nakacho and S. Endo, "A New Measuring Method of Residual Stress with the Aid of Finite Element Method and Reliability of Estimated Values", J. Soc. Naval Architects of Japan, Vol.138 (1975), 499-507 (in Japanese).
3) Y. Ueda, K. Fukuda and M. Tanigawa, "A New Measuring Method of Three Dimensional Stress Based on Theory of Inherent Strain", Trans. JWRI, Vol.8 (1979), No.2, 89-96, also Trans. ASME, J. Engineering Materials and Technology, Vol.111 (1989), 1-8.
4) T. Naka and T. Okumura, "Thermal Stress Due to Welding on the Thin Steel Plate (part I), J. Welding Soc., Vol.17 (1948), No.3, 2-12 (in Japanese).
5) M. Otani, "Graphical Solution of Thermal Stress by Welding (1 st Report)", J. Welding Soc., Vol.17 (1948), No.10, 3-12 (in Japanese).
6) M. Watanabe and K. Satoh, Trans. Soc. Naval Architects of Japan, Vol.86 (1954), (in Japanese).
7) Y. Ueda, E. Takahashi, K. Sakamoto and K. Nakacho, "Multipass Welding stress in Very Thick Plates and Their Reduction from Stress Relief Annealing", Trans. JWRI, Vol.5 (1976), No.2, 79-89.
8) Y. Ueda, K. Nakacho and T. Shimizu, "Improvement of Residual Stresses of Circumferential Joint of Pipe by Heat-Sink Welding", Trans. of ASME, J. Pressure Vessel Technology, Vol.108 (1986), 14-22.
9) Y. Ueda, K. Fukuda, Y. C. Kim and R. Koki, "Characteristics of Restraint Stress-Strain of Slit Weld in a Finite Rectangular Plate and the Significance of Restraint Intensities as a Dynamical Measure", Trans. JWRI, Vol.11 (1982), No.2, 105-113.
10) Y. Ueda, K. Fukuda, I. Nishimura, H. Iiyama, N. Chiba and M. Fukuda, "Three Dimensional Cold Bending and Welding Residual Stresses in Pen-stock of 80 kgf/mm^2 Class High Strength Steel Plate", Trans. JWRI, Vol.12 (1983), No.2, 117-126.
11) Y. Ueda and M. G. Yuan, "A Predicting Method of Welding Residual Stress Using Source of Residual Stress (Report III)", Trans. JWRI, Vol.22 (1993), No.1, 157-168, also Trans. ASME, J. Eng. Materials and Technology, Vol.115 (1993), 417-423.
12) Y. Ueda, N. X. Ma, Y. S. Wang and R. Koki, "Measurement of Residual Stresses in Single-pass and Multipass Fillet Welds Using Inherent Strains -Estimation and Measuring Methods of Residual Stresses Using Inherent Strain Distribution Described as Functions (Report V)", Quarterly J. Japan Welding Soc., Vol.13 (1995), No.3, 470-478.
13) Y. Ueda, H. Murakawa and N. X. Ma, "Measurement of Residual Stresses in Explosively Clad Steels and a Method of Residual Stress Reduction", Trans. JWRI, Vol.23 (1994), No.2, 249-255.
14) Y. Ueda and T. Yao, "The Influence of Complex Initial Deflection Modes on the Behavior and Ultimate Strength of Rectangular Plates in Compression", J. Constructional Steel Research, Vol.5 (1985), No.4, 265-302.
15) Y. Ueda and T. Yao, "Ultimate Strength of Stiffened plates and Minimum Stiffness Ratio of Their Stiffeners (under thrust), Trans. JWRI, Vol.10 (1981), No.2, 97-109.
16) Y. Ueda, H. Murakawa, S. M. Gu, Y. Okumoto and M. Nakamura, "Simulation of Welding Deformation for Accurate Ship Assembling (Report II) - Influence of Initial Geometrical Imperfection on Butt Welded Plate--", Trans. JWRI, Vol.22 (1993), No.1, 135-144.
17) Y. Ueda, H. Murakawa, S. M. Gu, Y. Okumoto and M. Ishiyama, "Simulation of Welding Deformation for Accurate Ship Assembling (Report III) - Out-of-plane Deformation of Butt Welded Plate -", Trans. Soc. Naval Architects of Japan, No.176 (1994), 341-350 (in Japanese).
18) Y. Ueda, H. Murakawa, S. M. Gu, Y. Okumoto and M. Ishiyama, "FEM Simulation of Gas and Plasma Cutting with Emphasis on Precision of Cutting", Trans. JWRI, Vol.23 (1994), No.1, 93-102.
19) Y. Ueda, J. Wang, H. Murakawa and M. G. Yuan, "Three Dimensional Numerical Simulation of Various Thermo-mechanical Processes by FEM (Report III)", Trans. JWRI, Vol.22 (1994), No.1, 127-134.
20) H. Murakawa, F. Kimura and Y. Ueda, "Weldability Analysis of Spot Welding on Aluminum Using FEM", Trans. JWRI, Vol.24 (1995), No.1, 101-111.
21) Y. Ueda, H. Murakawa, A. M. Rashwan, I. Neki, R. Kamichika, M. Ishiyama and J. Ogawa, "Development of Computer Aided Process Planning System for Plate Bending by Line-Heating (Report III) - Relation between Heating Condition and Deformation -", Trans. JWRI, Vol.22 (1993), No.1, 145-156.